1   **Title**: MicroRNAs expressed from FSHR and aromatase genes target important ovarian

2   functions [†]

3   **Running title**: Hsa-miR-548ba and hsa-miR-7973 target genes

4   **Summary sentence**: Confirmed targets of miRNAs hsa-miR-548ba and hsa-miR-7973 are

5   involved in follicle recruitment, apoptosis, intercellular interactions and extracellular matrix

6   remodeling pathways in KGN cells.

7

8   Ilmatar Rooda[1,2], Birgitta Kaselt[1], Andres Salumets[2,3,4,5], Agne Velthut-Meikas[1,2,*]

9

10   [1] Department of Chemistry and Biotechnology, Tallinn University of Technology, Tallinn,

11   Estonia

12   [2]Competence Centre on Health Technologies, Tartu, Estonia

13   [3]Institute of Clinical Medicine, Department of Obstetrics and Gynecology, University of Tartu,

14   Tartu, Estonia

15   [4]Institute of Biomedicine and Translational Medicine, Department of Biomedicine, University

16   of Tartu, Tartu, Estonia

17   [5]Department of Obstetrics and Gynecology, University of Helsinki and Helsinki University

18   Hospital, Helsinki, Finland

19

25   microarray data is available at Gene Expression Omnibus repository, accession number

26   GSE122731

27   * Correspondence: Department of Chemistry and Biotechnology, Tallinn University of

28   Technology, Akadeemia tee 15, 12618 Tallinn, Estonia; E-mail: agne.velthut@taltech.ee

Abstract

MicroRNAs (miRNAs) have known roles in the post-transcriptional regulation of various biological processes including ovarian follicle development. We have previously identified miRNAs from human pre-ovulatory granulosa cells that are expressed from the intronic regions of two key genes in normal follicular development: FSH receptor (FSHR) and CYP19A1, the latter encoding the aromatase enzyme. In the present study, we aim to identify the targets regulated by those two miRNAs: hsa-miR-548ba and hsa-miR-7973, respectively. The miRNAs of interest were endogenously expressed in KGN cell-line, gene expression changes were analyzed by Affymetrix microarray and confirmed by RT-qPCR. Potential miRNA-regulated sequences were further filtered from the obtained results by bioinformatic target prediction algorithms and validated for direct miRNA:mRNA binding by luciferase reporter assay. Our results verified Leukemia inhibitory factor receptor (LIFR), Phosphatase and tensin homolog (PTEN), Neogenin 1 (NEO1) and SP110 nuclear body protein (SP110) as target genes for hsa-miR-548ba. Hsa-miR-7973 target genes ADAM metallopeptidase domain 19 (ADAM19), Peroxidasin (PXDN) and Formin like 3 (FMNL3) also passed all verification steps. In conclusion we propose that hsa-miR-548ba may be involved in the regulation of follicle growth and activation via LIFR and PTEN. Hsa-miR-7973 may be implicated in the modulation of extracellular matrix and cell-cell interactions. Taken together, our results suggest that those two miRNAs of interest have important regulatory roles in granulosa cells and in follicle development in general.

Introduction

53 MicroRNAs (miRNAs) are short non-coding RNA molecules approximately 22 nucleotides in

54 length [1]. MicroRNAs bind to their target mRNA 3' untranslated region (3'UTR) at sites

55 complementary to the miRNA 5' seed region. MicroRNA biding to the target gene regulates

56 gene expression by destabilizing the mRNA and/or inhibiting its translation [2]. In a few cases,

57 an increase in gene expression has also been observed [3].

58 MicroRNAs have key role in the post-transcriptional regulation of various important

59 biological processes, including cell proliferation, differentiation, apoptosis, and hormone

60 biosynthesis and secretion [4]. Functional ovary requires precise coordination of follicle

61 recruitment, selection and ovulation processes. Development of ovarian follicles is a complex

62 process including oocyte maturation, granulosa cell proliferation and differentiation.

63 MicroRNAs expressed in the ovary have regulative roles in ovarian follicle development and

64 the expression of miRNAs in the ovary varies within the specific cell type and function [5].

65 The overall role of miRNAs in ovarian functions has been extensively studied in the mouse

66 models. *Dicer1* conditional knock-out mice without the ability to process mature miRNAs in

67 anti-Müllerian hormone expressing cells, including follicular granulosa cells, demonstrate

68 abnormalities in ovulation, early embryonic development, and estrous cycles [6].

69 Granulosa cell functions are essential in follicular development, maturation, and atresia.

70 Granulosa cells support oocyte growth via continuous bidirectional communication to ensure

71 oocyte quality and developmental competence. Due to the close communication cumulus

72 (CGC) and mural granulosa cells (MGC) may reflect the characteristics of the oocyte and an

73 understanding of the patterns of expression and functions of miRNAs in those cells may lead

74 to a better understanding of follicle maturation and its dysfunction [7,8]. Furthermore,

75 granulosa cell miRNAs may serve as potential biological markers that could be used to increase

76   the efficiency of assisted reproductive technologies by providing non-invasive means to assess

77   oocyte quality and embryo survival potential [7].

78   MicroRNAs hsa-miR-548ba and hsa-miR-7973 were previously identified by deep

79   sequencing of MGC and CGC populations isolated from women undergoing controlled ovarian

80   stimulation and in vitro fertilization. Both miRNAs are of intronic origin: hsa-miR-548ba gene

81   resides in the follicle stimulating hormone receptor (*FSHR*) gene and hsa-miR-7973 is located

82   in the intron of the *CYP19A1* gene [9]. The regulatory mechanisms and target genes for those

83   two miRNAs are currently not known.

84   Follicle stimulating hormone (FSH) activates time-related changes in granulosa cell

85   gene expression by binding to FSHR promoting proliferation, differentiation, antrum

86   formation, and oocyte maturation. Moreover, FSH stimulates aromatase expression and

87   estrogens production [10,11]. Estrogens are produced by aromatization of androgens by

88   aromatase enzyme encoded from *CYP19A1* gene [12]. Both FSHR and aromatase are crucial

89   for follicle development and maturation [11].

90   The aim of the current study was to identify the target genes of hsa-miR-548ba and hsa-

91   miR-7973 in human granulosa cells by using granulosa KGN cell line as a model [13]. The

92   genomic locations of the miRNAs of interest in FSHR and aromatase genes give a hypothesis

93   about important regulatory roles of these two miRNAs in granulosa cells regarding follicle

94   development and function.

95

96

Materials and methods

97

Cell culture of KGN cell line

98

99 Granulosa tumor-like cell line KGN was used as a model for cell line experiments [13]. Cells

100 were grown in L-glutamine-containing Dulbecco's Modified Eagle's medium with 10% fetal

101 bovine serum, 100U/ml penicillin and 0.1mg/ml streptomycin on 60x15mm culture plates at

102 37^oC and 5% CO_2. Cells were harvested with 0.05% trypsin and 0.02% EDTA (all solutions

103 from Naxo, Tartu, Estonia).

104

Isolation of primary granulosa cells

105

106 The study was approved by the Ethics Committee of the University of Tartu and an informed

107 consent was obtained from all participants. Granulosa cells were collected from eight women

108 undergoing intra-cytoplasmic sperm injection (ICSI) due to male-factor infertility. Ovarian

109 hormonal stimulation was conducted according to the GnRH antagonist (Cetrotide, Merck

110 Serono, Geneva, Switzerland) protocol with the administration of recombinant FSH (Gonal-F,

111 Merck Serono, or Puregon, Merck Sharp & Dohme Corp., Whitehouse Station, NJ, USA). All

112 patients underwent ovarian puncture (OPU) of follicles ≥15 mm in size after 36 h of hCG

113 administration (Ovitrelle, Merck Serono).

114 MGCs were obtained from follicular fluid after OPU following the manual removal of

115 cumulus-oocyte complexes and CGC aggregates devoid of the oocyte. The fluid from all

116 follicles of a patient was pooled, centrifuged at $450g$ for 10 minutes, followed by supernatant

117 removal. The cells were separated on a 50% density gradient of PureSperm 100 (Nidacon;

118 Mölndal, Sweden) in Universal IVF Medium (Origio; Jyllinge, Denmark), washed three times

119 in Universal IVF Medium at $37°C$, depleted of CD45-positive leukocytes according to the

120 manufacturer's suggested protocol (DynaMag and Dynabeads; Life Technologies, Carlsbad,

121   California), lysed with QIAGEN miRNeasy Mini kit lysis buffer (QIAGEN, Hilden,

122   Germany), and stored in liquid nitrogen for future use.

123   CGC were collected 4 h after OPU during oocyte denudation lasting up to 5 min with

124   type IV-S hyaluronidase extracted from bovine testes (Sigma-Aldrich, St-Louis, MO, USA)

125   and diluted in Sperm Preparation Medium (Origio). The CGC from all oocytes irrespective of

126   their maturity were pooled and centrifuged at 450g for 5 min, the supernatant was discarded,

127   and the cells were lysed and stored as described above.

128

129   **Cell line transfection**

130   For microRNA transfection Lipofectamine RNAiMAX reagent (Invitrogen, Carlsbad, C

131   A) and miRCURY LNA miRNA mimics hsa-miR-548ba, hsa-miR-7973 and control miRNA

132   with no mammalian homologue cel-miR-39-3p [14,15] were used according to manufacturer's

133   protocol (Exiqon, Vedbaek, Denmark). MicroRNA mimics were transfected at previously

134   optimized concentration of 12.5nM and 72 h time-point after transfection was tested.

135   For miRNA and luciferase vector co-transfection Lipofectamine 2000 reagent

136   (Invitrogen) and previously specified miRCURY LNA miRNA mimics were used according

137   to manufacturer's protocol. MicroRNA final concentration in culture medium was 12.5nM or

138   50nM, while 100ng of vector was transfected.

139

140   **Cytotoxicity analysis**

141   MicroRNA cytotoxicity analysis was performed using CytoTox-Glo Cytotoxicity Assay

142   (Promega Corporation, Madison, Wisconsin, USA) according to the user manual. Five

143   thousand cells were plated in each well of a white Greiner CELLSTAR 96-well plate (Sigma-

144   Aldrich, St-Louis, MO, USA) and transfection was performed 24 h after plating. Non-

145   transfected control samples were measured at 0, 24, 48, and 72 h. The cytotoxicity of cells

146 transfected with either hsa-miR-548ba, hsa-miR-7973 or cel-miR-39-3p mimics was measured

147 at 24, 48 and 72 h post-transfection. The above-mentioned assay uses a luminogenic peptide

148 substrate to measure dead-cell protease activity, which is released from cells upon losing their

149 membrane integrity. Luminescence was measured in two steps with Tecan GeniosPro

150 luminometer (Tecan, Männedorf, Switzerland). Firstly, luminescence from dead cells and

151 secondly luminescence from all cells after lysis was detected. Results were calculated as

152 luminescence from all lysed cells minus luminescence from dead cells. All samples were

153 measured in triplicates and the average value of three independent experiments was used in

154 data analysis.

155

156 **RNA extraction**

157 Cells were lysed in QIAzol lysis reagent (QIAGEN). For total RNA extraction miRNeasy Mini

158 Kit (QIAGEN) was used. In addition, small fraction RNA (≤200 nucleotides) extraction was

159 performed separately using RNeasy Mini Elute Cleanup Kit (QIAGEN). Both total and small

160 RNA extraction was performed according to the user manual. RNA concentrations were

161 measured using NanoDrop 2000c spectrophotometer (Thermo Fisher Scientific, Dreieich,

162 Germany).

163 The quality of all RNA samples analyzed on Affymetrix microarray was evaluated

164 using the Agilent 2100 Bioanalyzer system (Agilent Technologies, Waldbronn, Germany). All

165 RNA samples were of high quality, with the RNA Integrity Number values between 9.2-9.8.

166

167 **Affymetrix microarray**

168 Affymetrix microarray was performed at the Array and Analysis Facility at Uppsala

169 Biomedical Center, Sweden. From each sample 250ng of total RNA were used to generate

170 amplified and biotinylated sense-strand cDNA according to the GeneChip WT PLUS Reagent

171   Kit User manual (Affymetrix, Santa Clara, CA). GeneChip Human Gene 2.0 ST Arrays were

172   hybridized for 16h in 45°C incubator, rotated at 60rpm. Arrays were washed and stained using

173   the Fluidics Station 450 and scanned using GeneChip® Scanner 3000 7G. Affymetrix

174   microarray data is available at Gene Expression Omnibus repository, accession number

175   GSE122731.

176

177   **Reverse transcription**

178   For cDNA synthesis from mRNA SuperScript III First Strand Synthesis SuperMix (Invitrogen)

179   was used according to user manual. 1µg of cell line and 500ng of primary granulosa cell RNA

180   was used as input.

181   For microRNA detection cDNA was synthesized using miRCURY LNA^{TM} Universal

182   RT microRNA PCR Universal cDNA Synthesis Kit III (Exiqon). 200ng of small fraction RNA

183   was used as input.

184

185   **Primer design**

186   Primers used for RT-qPCR analysis were designed using NCBI primer-BLAST

187   (http://www.ncbi.nlm.nih.gov/tools/primer-blast/). Preferred primers spanned exon-exon

188   junctions and amplified all splice isoforms of the given gene. Primer sequences are presented

189   in Supplementary Table IA.

190   Primers for amplifying the 3'UTR sequences of potential miRNA target genes were

191   designed in Benchling (https://benchling.com/). Primer binding specificity was tested using

192   NCBI primer-BLAST (Supplementary Table IB).

193

194 **RT-qPCR**

195 The RT-qPCR analysis was carried out using SDS 2.3 software in 7900HT Fast Real-Time

196 PCR System (Applied Biosystems, Foster City, California). For the detection of mRNA

197 expression, Platinum SYBR Green qPCR SuperMix-UDG (Invitrogen) or Platinum SYBR

198 Green qPCR SuperMix-UDG with ROX (Invitrogen) was used. cDNA from small RNA

199 fraction was amplified by EXILENT SYBR Green Mastermix (Exiqon) according to the user

200 manual. Each sample was run in triplicates on a 384-well plate. The specificity of amplified

201 PCR products was determined by melt curve analysis.

202

203 **Luciferase reporter vector cloning and luciferase assay**

204 The full length 3'UTR of hsa-miR-548ba potential target genes *BCL2L11*, *LIFR*, *NEO1*, *PTEN*,

205 *RARB*, *SP110*, hsa-miR-7973 target genes *ADAM19*, *ATHL1*, *ATP6V1A*, *PXDN*, *FMNL3*, and

206 the common target for both miRNAs *TGFBR2* were cloned into pmirGLO Dual-Luciferase

207 vector (Promega) downstream of the Firefly luciferase gene. Target gene 3'UTR sequences

208 were obtained from UCSC Genome Browser (https://genome.ucsc.edu/) with an exception of

209 *FMNL3* where shorter isoform of 3'UTR was used. Bioinformatic prediction program

210 TargetScan 7.1 [16] uses *FMNL3* 3'UTR isoform with length 7,874 nt, while in UCSC Genome

211 Browser the length is 9,316 nt. Moreover, for *PTEN* also a shorter version of 3'UTR isoform

212 was cloned which is used by miRDB bioinformatical target prediction program [17]. Potential

213 target gene 3'UTR sequences and predicted miRNA binding sites are available in

214 Supplementary Material. Primers for amplifying full length 3'UTR from genomic KGN cell

215 line DNA and restriction enzymes used for cloning are presented in Supplementary Table IB.

216 Validation of hsa-miR-548ba and hsa-miR-7973 direct binding to target gene 3'UTR

217 was performed by using Dual-Glo Luciferase assay system (Promega) according to the user

218 manual. Luciferase signal was measured 24 h after miRNA and vector co-transfection. The

219 relative luciferase activities were determined by calculating the ratio of Firefly luciferase

220 activities over Renilla luciferase activities. All experiments were repeated three times as

221 triplicates on a white Greiner CELLSTAR 96-well plate (Sigma-Aldrich). Cel-miR-39-3p was

222 used as a negative control.

223

224 **Data analysis and statistics**

225   **a. Affymetrix microarray data analysis**

226 Affymetrix microarray raw data was normalized in Expression Console, provided by

227 Affymetrix (http://www.affymetrix.com), using the robust multi-array average (RMA)

228 method. Differential gene expression analysis was carried out in the statistical computing

229 language R (http://www.r-project.org) using packages available from the Bioconductor project

230 (www.bioconductor.org) [18]. To detect differentially expressed genes between samples

231 transfected with hsa-miR-548ba or hsa-miR-7973 and cel-miR-39-3p groups, an empirical

232 Bayes moderated t-test was applied using the "limma" package [19]. The p-values were

233 adjusted for multiple testing according to the method of Benjamini and Hochberg [20].

234 Statistical significance level was set at adjusted $p < 0.01$.

235   For cluster analysis of microarray data genes were ordered by the highest fold change

236 expression difference upon hsa-miR-548ba transfection and Bioconductor package "heatmap"

237 was used.

238   **b. Gene ontology analysis**

239 Analysis of over- and under-representation of Reactome pathways (version 58) was performed

240 in the Panther classification system [21]. Genes differentially expressed (adjusted $p < 0.01$) on

241 Affymetrix microarray upon transfecting KGN cells with either hsa-miR-548ba or hsa-miR-

242 7973 mimics compared to the transfection with cel-miR-39-3p were used as input. Fisher's

243 exact test with Benjamini and Hochberg false-discovery rate (FDR) correction was used to test

244 the statistical significance of the results and over- or under-represented pathways obtaining

245 FDR < 0.05 are reported.

c. MicroRNA target gene prediction

247 For miRNA bioinformatic target prediction four web based programs were used (DIANA

248 microT v 3.0 [22], microT CDS v5.0 [23], TargetScan 7.1 [16] and miRDB [17]). Gene was

249 considered as a potential miRNA target in case it was predicted by at least two programs out

250 of four and its gene expression fold change according to microarray analysis was $\geq \log_2(|0.3|)$.

d. RT-qPCR

252 The gene-specific mRNA expression Ct values were normalized against *GAPDH* expression

253 and miRNA expression levels were normalized for internal control hsa-miR-132-3p using the

254 $2^{-\Delta\Delta Ct}$ method of relative quantification [24]. Experiments were run in technical triplicates three

255 times. Results are shown as average ± SD (standard deviation). Statistical significance was

256 calculated by two-tailed Student t-test in Microsoft Office Excel 2017. Statistical significance

257 level was set at $p < 0.05$.

e. Luciferase assay

259 The relative luciferase activities were determined by calculating the ratio of Firefly luciferase

260 relative light units (RLU) over Renilla luciferase RLU. All experiments were run

261 independently three times as triplicates. Results are shown as average ± SE (standard error).

262 Statistical significance was calculated by one-tailed Student t-test in Microsoft Office Excel

263 2017. Statistical significance level was set at $p < 0.05$.

264

265

266

Results

Global gene expression changes upon transient expression of hsa-miR-548ba and hsa-miR-7973 in KGN cells

The first aim of the current study was to evaluate the effect of miRNA transfection on the global gene expression change in human granulosa cell line KGN. In non-transfected KGN cells the expression levels of hsa-miR-548ba and hsa-miR-7973 barely reached the detection limit (Supplementary Figure 1). After optimization experiments (data not shown), the transfection of 12.5nM miRNA mimic lead to considerably higher expression levels in comparison to primary granulosa cells (Supplementary Figure 1). However, such level of over-expression did not influence cell viability or proliferation rate (Supplementary Figure 2).

Genome-wide gene expression changes upon miRNA transfection were studied on Affymetrix GeneChip Human Gene 2.0 ST Array. The results demonstrated that upon hsa-miR-548ba transfection the expression level of 1,474 and upon hsa-miR-7973 the expression level of 1,552 genes changed with statistical significance (adjusted p-value <0.01, Supplementary Table IIA and IIC). From those genes 1,015 were regulated by both miRNAs, 459 genes only by hsa-miR-548ba and 537 by hsa-miR-7973. Gene expression changes were calculated as compared to the control samples transfected with miRNA cel-miR-39-3p that presumably has no target sequences in human cells.

Cluster analysis of microarray results revealed that control samples expressing cel-miR-39-3p grouped separately from samples transfected with hsa-miR-548ba and hsa-miR-7973 (Figure 1). Cells expressing the human miRNAs under study had more similar gene expression patterns compared to samples transfected with cel-miR-39-3p. This is also confirmed by the overlapping number of commonly regulated genes.

Transfection of KGN cells with hsa-miR-548ba and hsa-miR-7973 leads to the regulation of several common as well as unique signaling pathways (Supplementary Table IIIA

292   and IIIB). Genes differentially expressed upon hsa-miR-548ba transfection are over-

293   represented in syndecan interactions, glycosaminoglycan and fatty acid metabolism, unfolded

294   protein response, G protein-coupled receptor (GPCR) and ephrin signaling among others

295   (Supplementary Table IIIA). Expression of hsa-miR-7973 in KGN cells resulted in the

296   regulation of genes involved in signaling by netrin-1, EGFR, PDGF, and TGF-beta receptor

297   complex, as well as pathways related to the immune system (Supplementary Table IIIB). As

298   several genes were regulated by both miRNAs, common targeted pathways include cholesterol

299   biosynthesis and amino acid transport across cell membrane (Supplementary Table IIIA and

300   IIIB).

301

302   **Bioinformatic target prediction**

303   Microarray analysis results may partly demonstrate secondary effects on mRNA expression:

304   gene expression changes triggered by primary miRNA targets. Therefore, to discriminate

305   between primary and secondary target genes the differential expression results obtained from

306   the microarray analysis method were compared to potential miRNA target mRNA-s predicted

307   by bioinformatic algorithms. However, bioinformatic prediction may also provide false

308   positive hits. In order to minimize such false positive findings, four target prediction programs

309   were used: DIANA microT v 3.0 [22], microT CDS v5.0 [23], TargetScan 7.1 [16] and miRDB

310   [17]. A gene was considered as a potential true target for a miRNA when it was positively

311   predicted by at least two programs out of four.

312   The overlap of statistically significant microarray results and bioinformatically

313   predicted target genes are presented in Supplementary Table IIB and IID. Shortly, hsa-miR-

314   548ba and hsa-miR-7973 potentially target the mRNA-s of 76 and 58 genes, respectively. Both

315   miRNAs also share one common target mRNA of *TGFBR2* gene.

316

Validation of microarray results by RT-qPCR

Sixteen potential target genes from the overlapping list of microarray and bioinformatic target prediction results were validated by RT-qPCR: 8 potential targets of hsa-miR-548ba and 7 of hsa-miR-7973 and their common target *TGFBR2*. The list of validated genes was selected according to published data linking the molecular functions of these proteins to their potential importance in folliculogenesis (Table I). As a result, *BCL2L11*, *LIFR*, *NEO1, PTEN* and *SP110* were statistically significantly down-regulated at mRNA level upon cell transfection with hsa-miR-548ba mimic (Figure 2A). *RARB* was down-regulated with borderline statistical significance (p=0.057, Figure 2A). From the list of potential hsa-miR-7973 targets the expression levels of *ADAM19*, *ATHL1*, *ATP6V1A, FMNL3* and *PXDN* were statistically significantly decreased (Figure 2B). The expression change of the common target gene *TGFBR2* was confirmed only in case of hsa-miR-7973 transient expression (Figure 2B).

MicroRNA target binding validation by luciferase reporter assay

Potential miRNA targets that demonstrated significant gene expression change by microarray (p < 0.01) and RT-qPCR methods (p < 0.05) were further validated for direct miRNA:mRNA binding by luciferase reporter assay. Shortly, hsa-miR-548ba potential target genes: *BCL2L11*, *LIFR*, *NEO1, PTEN, RARB* and *SP110*, and hsa-miR-7973 target genes: *ADAM19*, *ATHL1*, *ATP6V1A*, *FMNL3* and *PXDN*. Although *TGFBR2* gene expression change was not confirmed by RT-qPCR in hsa-miR-548ba transfected cells, binding of its 3'UTR to both miRNAs under study was nevertheless assessed.

Potential target gene *PTEN* was tested with two versions of 3'UTR lengths: 3'UTR length obtained from UCSC Genome browser and second from miRDB bioinformatical prediction program, marked as *PTEN* long and *PTEN* short, respectively. pmirGLO-3'UTR-PTEN vector and hsa-miR-21-5p were used as a positive control for miRNA:mRNA binding

342 to confirm our luciferase assay reliability as *PTEN* has been previously shown to be a target

343 for hsa-miR-21-5p [41]. Upon direct binding of miRNA to the 3'UTR sequence of its target

344 mRNA, reduction in the measured luciferase signal is expected. Such suppression of luciferase

345 signal upon hsa-miR-21-5p binding to *PTEN* 3'UTR is demonstrated in Supplementary Figure

346 3 for both long and short variants.

347 Luciferase assay results confirmed the direct binding of hsa-miR-548ba to *LIFR,*

348 *NEO1*, *PTEN* and *SP110* 3'UTR sequences. Hsa-miR-548ba bound to its potential target *PTEN*

349 3'UTR sequence only when the longer version was used (Figure 3A). From the tested potential

350 targets of hsa-miR-7973 direct binding occurred on the 3'UTR of *ADAM19*, *FMNL3* and

351 *PXDN* (Figure 3B).

352

Discussion

354 Here we present the first functional analysis of miRNAs hsa-miR-548ba and hsa-miR-7973 by

355 identifying their target genes in KGN cells using Affymetrix microarray, RT-qPCR and

356 luciferase assay.

357 The miRNAs of interest: hsa-miR-548ba and hsa-miR-7973, were both identified for

358 the first time from human ovaries by deep sequencing approach of primary granulosa cells [9].

359 In the described functional experiments we used granulosa tumor-like KGN cell line as

360 granulosa cell model that has been previously used to understand the regulation of

361 steroidogenesis, cell growth and apoptosis in human granulosa cells [13]. KGN cells express

362 functional FSH receptor and high level of aromatase, encoded from miRNA hsa-miR-548ba

363 and hsa-miR-7973 host genes *FSHR* and *CYP19A1*, respectively. KGN cell line has also been

364 previously used for miRNA target identification and luciferase assay studies for direct

365 miRNA:mRNA interactions [42].

366   MicroRNAs are estimated to regulate 60% of all protein-coding genes and a single

367   miRNA may regulate up to 400 different target mRNAs [43]. Our microarray results

368   demonstrated 1,474 differentially expressed genes upon hsa-miR-548ba transfection, and

369   1,552 genes potentially regulated by hsa-miR-7973. From differentially expressed genes 1,015

370   were regulated by both miRNAs, 459 genes only by hsa-miR-548ba and 537 by hsa-miR-7973.

371   Gene ontology analysis from hsa-miR-548ba regulated genes showed enrichment in fatty acid

372   metabolism and ephrin signaling pathways and over-expression of hsa-miR-7973 showed

373   enrichment in TGF beta receptor complex and immune system pathways. Commonly regulated

374   genes by these two miRNAs targeted cholesterol biosynthesis pathway. Cholesterol is a major

375   component for steroidogenesis and sources of cholesterol for ovarian granulosa cells include

376   plasma lipoproteins and de novo-synthesis [44]. Therefore, the regulation of cholesterol

377   biosynthesis pathway by the miRNAs under study may influence steroid hormone production,

378   contributing to the follicular developmental stage-dependent estradiol and progesterone

379   production.

380   Although, miRNAs may regulate several hundreds of target genes, microarray results

381   do not differentiate primary targets from secondary regulatory effects: i.e. the genes regulated

382   by primary miRNA targets. Such secondary regulatory effects are common in over-expression

383   conditions and large data-sets obtained by genome-wide methods like microarray gene

384   expression analysis [45]. The large number of commonly regulated genes by both miRNAs

385   analyzed in the present study can be also explained by secondary effects on gene expression,

386   as miRNA transfection and over-expression can potentially lead to the saturation of RNA

387   silencing complex (RISC) which results with altered gene expression regulation [46].

388   Moreover, miRNAs may target transcription factors influencing the expression of a number of

389   secondary target genes [45]. To better distinguish primary miRNA targets from secondary

390   ones, microarray results were compared to bioinformatically predicted target genes.

391   MicroRNAs are known to have regulatory roles in many stages of follicle development

392   and granulosa cell functions [5]. To investigate the role of the two miRNAs of interest, the

393   overlapping part of microarray and bioinformatically predicted potential targets were filtered

394   for genes with a known role in ovarian function and tested for miRNA:mRNA binding effects

395   on protein expression.

396   For direct miRNA:mRNA binding and protein expression studies luciferase assay

397   reporter vectors were cloned with potential target gene 3'UTR sequences. In this study full

398   length 3'UTR sequences were used, except for *PTEN* in case of which bioinformatic prediction

399   algorithms do not use consistent 3'UTR sequence lengths and thus two different sequences

400   were used. We chose to test full-length sequences for most of the target genes as we lacked the

401   knowledge of functional miRNA target regions and the exact biding site identification within

402   each potential target gene was not the goal of the current study. Furthermore, the secondary

403   structure of 3'UTR could also determine the accessibility of miRNA binding leading to our

404   choice of using full length 3'UTRs. Testing a fragment of 3'UTR may easily lead to false

405   results due to the different secondary structure from the full length sequence [47]. Furthermore,

406   3'UTR central regions are more likely to be incorporated to hairpin structures which could lead

407   to concealing the target sites of miRNAs. This is also supported by different binding site

408   efficiencies: miRNA sites near the ends of the 3'UTR are more effective than sites in the center

409   of the 3'UTR [47,48]. Direct binding assay confirmed *LIFR*, *PTEN*, *NEO1* and *SP110* as hsa-

410   miR-548ba targets. For target gene *PTEN* direct binding occurred only with the longer 3'UTR

411   sequence, although bioinformatic algorithms used in this work predicted target sequences into

412   the shorter 3'UTR isoform. Such results can be explained by the differences in the secondary

413   structure mentioned above. Moreover, bioinformatical programs may not predict all the

414   potential target sequences for miRNA hsa-miR-548ba. Taken together, target gene 3'UTR

415   length is critical for miRNA binding to its target sequences in direct binding assays.

416   LIFR is a receptor for leukemia inhibitory factor (LIF). LIF has been shown to promote

417   primordial to primary follicle transition in the rat ovary [49]. In cattle, follicle atresia is

418   regulated by LIF-STAT3 pathway which can be reversed with FSH administration [50]. In

419   humans, the role of LIF and its receptor in the ovary is not well characterized, but LIF and

420   LIFR mRNA expression in human ovarian samples are consistent with the concept that LIF

421   might be involved in growth initiation of human primordial follicles through its receptor [28].

422   Second direct target gene for hsa-miR-548ba, *PTEN*, is involved in primordial follicle

423   dormancy and activation. The recruitment of primordial follicles is regulated by highly

424   controlled mechanisms and the critical role held by PI3K-Akt signaling pathway. This pathway

425   is negatively regulated by PTEN and it is showed that in mice lacking *PTEN* the entire

426   primordial follicle pool becomes activated [30]. In bovine the levels of PI3K-Akt signaling

427   pathway components in MGC and CGC have a correlation with oocyte competence. Decreased

428   PTEN expression and increased expression of PTEN downregulating miRNAs lead to the

429   activation of PI3K-Akt pathway and correlates with the number of high-quality oocytes [51].

430   Therefore, the timing of PTEN expression regulation is important for follicle development and

431   oocyte competence. Although hsa-miR-548ba expression pattern throughout the follicle

432   development is currently unknown, a similar regulation of PTEN by hsa-miR-548ba may have

433   an important role in the determination of oocyte developmental competence.

434   NEO1 is a member of immunoglobulin superfamily and is a receptor for repulsive

435   guidance molecules, netrins, and is involved in bone morphogenetic protein (BMP) signaling

436   pathways by directly binding BMPs [29]. Moreover, NEO1 activates RAC1-PI3K-AKT

437   signaling pathway in human gastric cancer cells [52]. In mouse ovary, Rac1 is involved in

438   primordial follicle formation by inducing nuclear transport of SMAD3 [53]. As mentioned

439   above, PI3K-AKT signaling pathway have crucial roles to balance follicle growth suppression,

440   activation and progression also in humans [54] and BMPs have important role in follicle

441 development including primordial germ cell development, oocyte-somatic cell interactions and

442 modulating of COC formation and expansion [55].

443   The role of SP110 in the ovary is less clear. It has been suggested that SP110 may

444 function as a nuclear hormone receptor transcriptional coactivator via binding to the retinoic

445 acid receptor alpha (RARA) response element [32]. Retinoids are essential for steroid

446 production and it has been demonstrated that bovine CGCs express active RARA [56]. The

447 role of SP110 in human granulosa cells has to be further investigated, but SP110 regulation by

448 miRNA hsa-miR-548ba may influence retinoid signalization.

449   Moreover, direct hsa-miR-548ba targets *PTEN*, *NEO1* and potential secondary target

450 *BCL2L11* are also involved in regulating apoptosis [25,57,58]. However, the role of hsa-miR-

451 548ba in modulating apoptotic pathways in the human ovary needs to be investigated further.

452 In the current study, exogenous expression of hsa-miR-548ba did not lead to changes in overall

453 cellular viability during 72 h. Studies involving long-term ovarian culture conditions could

454 shed more light on the importance of hsa-miR-548ba on cell viability.

455   The confirmed targets of hsa-miR-7973 according to our study were *ADAM19*, *PXDN*

456 and *FMNL3*, all of which have been shown to be involved in ECM modulation and cell-cell

457 interactions [33,38]. ADAM19 cleaves extracellular matrix (ECM) proteins, growth factors

458 and cytokines like neuregulin and plays an essential role in embryo implantation by remodeling

459 ECM [33]. Neuregulin 1 (NRG1) is expressed in granulosa cells and induced by luteinizing

460 hormone (LH). NRG1 regulates the meiotic resumption time of the oocyte leading to proper

461 oocyte maturation and developmental competence in cultured COCs [59]. The down-regulation

462 of ADAM19 expression by miRNA hsa-miR-7973 could lead to lower cleavage rate of NRG1.

463 Therefore, it is important to know the timing of miRNA hsa-miR-7973 regulation of ADAM19

464 and how this influences NRG1 cleavage levels.

465   PXDN is a peroxidase previously investigated in the context of ovarian cancer where

466   the knockdown of this gene inhibits cellular proliferation, invasion and migration of ovarian

467   cancer cells [38]. Moreover, PXDN may promote proliferation of ovarian cancer cells by

468   regulating the activity of PI3K-AKT signaling pathway [38]. The role of PXDN in follicular

469   cells still needs further clarification.

470   Regulation of FMNL3 is not previously investigated in the context of ovary but this

471   protein has been shown to be involved in cytoskeletal organization, cell morphology, migration

472   and cell-cell adhesion [36,60].

473   Genes with negative results from luciferase assay can be considered as secondary

474   targets of miRNAs of interest but we have to keep in mind that the experiments were performed

475   with reporter vectors and in cell line conditions that may not fully reflect physiological

476   conditions in primary cells. Negative binding results may be the outcome of multiple biological

477   reasons. For example, miRNA target recognition may require multiple transacting factors

478   which leads to targeting only in specific cellular contexts. Also the alternative polyadenylation

479   of 3'UTRs in reporter vectors may increase the false-negative results [61]. In addition, many

480   possible target genes were excluded in this study due to the negative result from microarray

481   gene expression analysis using the cell line model and were thus not tested in the direct binding

482   assay. Therefore, in another experimental setting those genes may still be proven as direct

483   targets, leading to the conclusion that the list of validated target genes for these two miRNAs

484   of interest is not final.

485   Overall, we confirmed several targets for miRNA hsa-miR-548ba and hsa-miR-7973.

486   According to the previously known functions of their target genes we suggest that those two

487   miRNAs may have potential regulatory roles in granulosa cell gene expression and in follicle

488   development in general.

489

490 **Acknowledgments**

491 We are thankful to professor Markku Heikinheimo from the Institute of Clinical Medicine,

492 University of Helsinki for providing KGN cell-line for this project. We thank Hanna Göransson

493 Kultima, from the Array and Analysis Facility, SciLifeLab Uppsala, Sweden for her assistance

494 in microarray data analysis.

References

[1] Lee RC, Feinbaum RL, Ambros V. The C. elegans heterochronic gene lin-4 encodes small RNAs with antisense complementarity to lin-14. Cell 1993; 75:843–854.

[2] Bartel DP. MicroRNA Target Recognition and Regulatory Functions. Cell 2009; 136:215–233.

[3] Vasudevan S, Tong Y, Steitz JA. Switching from Repression to Activation: MicroRNAs Can Up-Regulate Translation. Science 2007; 318:1931–1934.

[4] Li Y, Fang Y, Liu Y, Yang X. MicroRNAs in ovarian function and disorders. J Ovarian Res 2015; 8.

[5] Maalouf SW, Liu WS, Pate JL. MicroRNA in ovarian function. Cell Tissue Res 2016; 363:7–18.

[6] Nagaraja AK, Andreu-Vieyra C, Franco HL, Ma L, Chen R, Han DY, Zhu H, Agno JE, Gunaratne PH, DeMayo FJ, Matzuk MM. Deletion of Dicer in somatic cells of the female reproductive tract causes sterility. Mol Endocrinol Baltim Md 2008; 22:2336–2352.

[7] D'Aurora M, Sperduti S, Di Emidio G, Stuppia L, Artini PG, Gatta V. Inside the granulosa transcriptome. Gynecol Endocrinol Off J Int Soc Gynecol Endocrinol 2016; 32:951–956.

[8] Uyar A, Torrealday S, Seli E. Cumulus and granulosa cell markers of oocyte and embryo quality. Fertil Steril 2013; 99.

[9] Velthut-Meikas A, Simm J, Tuuri T, Tapanainen JS, Metsis M, Salumets A. Research resource: small RNA-seq of human granulosa cells reveals miRNAs in FSHR and aromatase genes. Mol Endocrinol Baltim Md 2013; 27:1128–1141.

[10] Oktay K, Briggs D, Gosden RG. Ontogeny of Follicle-Stimulating Hormone Receptor Gene Expression in Isolated Human Ovarian Follicles. J Clin Endocrinol Metab 1997; 82:3748–3751.

[11] Ulloa-Aguirre A, Zariñán T, Pasapera AM, Casas-González P, Dias JA. Multiple facets of follicle-stimulating hormone receptor function. Endocrine 2007; 32:251–263.

[12] Miller WL, Auchus RJ. The Molecular Biology, Biochemistry, and Physiology of Human Steroidogenesis and Its Disorders. Endocr Rev 2011; 32:81–151.

[13] Nishi Y, Yanase T, Mu Y, Oba K, Ichino I, Saito M, Nomura M, Mukasa C, Okabe T, Goto K, Takayanagi R, Kashimura Y, et al. Establishment and characterization of a steroidogenic human granulosa-like tumor cell line, KGN, that expresses functional follicle-stimulating hormone receptor. Endocrinology 2001; 142:437–445.

[14] Mitchell PS, Parkin RK, Kroh EM, Fritz BR, Wyman SK, Pogosova-Agadjanyan EL, Peterson A, Noteboom J, O'Briant KC, Allen A, Lin DW, Urban N, et al. Circulating microRNAs as stable blood-based markers for cancer detection. Proc Natl Acad Sci 2008; 105:10513–10518.

[15] Schlosser K, Taha M, Stewart DJ. Systematic Assessment of Strategies for Lung-targeted Delivery of MicroRNA Mimics. Theranostics 2018; 8:1213–1226.

[16] Agarwal V, Bell GW, Nam J-W, Bartel DP. Predicting effective microRNA target sites in mammalian mRNAs. ELife 2015; 4:e05005.

[17] Wong N, Wang X. miRDB: an online resource for microRNA target prediction and functional annotations. Nucleic Acids Res 2015; 43:D146–D152.

[18] Huber W, Carey VJ, Gentleman R, Anders S, Carlson M, Carvalho BS, Bravo HC, Davis S, Gatto L, Girke T, Gottardo R, Hahne F, et al. Orchestrating high-throughput genomic analysis with Bioconductor. Nat Methods 2015; 12:115–121.

542 [19] Ritchie ME, Phipson B, Wu D, Hu Y, Law CW, Shi W, Smyth GK. limma powers
543   differential expression analyses for RNA-sequencing and microarray studies. Nucleic
544   Acids Res 2015; 43:e47.
545 [20] Benjamini Y, Hochberg Y. Controlling the False Discovery Rate: A Practical and
546   Powerful Approach to Multiple Testing. J R Stat Soc Ser B Methodol 1995; 57:289–
547   300.
548 [21] Mi H, Muruganujan A, Casagrande JT, Thomas PD. Large-scale gene function analysis
549   with the PANTHER classification system. Nat Protoc 2013; 8:1551–1566.
550 [22] Maragkakis M, Alexiou P, Papadopoulos GL, Reczko M, Dalamagas T, Giannopoulos
551   G, Goumas G, Koukis E, Kourtis K, Simossis VA, Sethupathy P, Vergoulis T, et al.
552   Accurate microRNA target prediction correlates with protein repression levels. BMC
553   Bioinformatics 2009; 10:295.
554 [23] Reczko M, Maragkakis M, Alexiou P, Grosse I, Hatzigeorgiou AG. Functional
555   microRNA targets in protein coding sequences. Bioinforma Oxf Engl 2012; 28:771–
556   776.
557 [24] Livak KJ, Schmittgen TD. Analysis of relative gene expression data using real-time
558   quantitative PCR and the 2(-Delta Delta C(T)) Method. Methods San Diego Calif 2001;
559   25:402–408.
560 [25] Concannon CG, Tuffy LP, Weisová P, Bonner HP, Dávila D, Bonner C, Devocelle MC,
561   Strasser A, Ward MW, Prehn JHM. AMP kinase–mediated activation of the BH3-only
562   protein Bim couples energy depletion to stress-induced apoptosis. J Cell Biol 2010;
563   189:83–94.
564 [26] Munkley J, Vodak D, Livermore KE, James K, Wilson BT, Knight B, Mccullagh P,
565   Mcgrath J, Crundwell M, Harries LW, Leung HY, Robson CN, et al. Glycosylation is
566   an Androgen-Regulated Process Essential for Prostate Cancer Cell Viability.
567   EBioMedicine 2016; 8:103–116.
568 [27] Kranc W, Brązert M, Ożegowska K, Nawrocki MJ, Budna J, Celichowski P,
569   Dyszkiewicz-Konwińska M, Jankowski M, Jeseta M, Pawelczyk L, Bruska M, Nowicki
570   M, et al. Expression Profile of Genes Regulating Steroid Biosynthesis and Metabolism
571   in Human Ovarian Granulosa Cells—A Primary Culture Approach. Int J Mol Sci 2017;
572   18.
573 [28] Abir R, Fisch B, Jin S, Barnnet M, Freimann S, Van den Hurk R, Feldberg D, Nitke S,
574   Krissi H, Ao A. Immunocytochemical detection and RT–PCR expression of leukaemia
575   inhibitory factor and its receptor in human fetal and adult ovaries. MHR Basic Sci
576   Reprod Med 2004; 10:313–319.
577 [29] Hagihara M, Endo M, Hata K, Higuchi C, Takaoka K, Yoshikawa H, Yamashita T.
578   Neogenin, a Receptor for Bone Morphogenetic Proteins. J Biol Chem 2011; 286:5157–
579   5165.
580 [30] Reddy P, Liu L, Adhikari D, Jagarlamudi K, Rajareddy S, Shen Y, Du C, Tang W,
581   Hämäläinen T, Peng SL, Lan Z-J, Cooney AJ, et al. Oocyte-Specific Deletion of Pten
582   Causes Premature Activation of the Primordial Follicle Pool. Science 2008; 319:611–
583   613.
584 [31] Udhane SS, Pandey AV, Hofer G, Mullis PE, Flück CE. Retinoic acid receptor beta and
585   angiopoietin-like protein 1 are involved in the regulation of human androgen
586   biosynthesis. Sci Rep 2015; 5.
587 [32] Bloch DB, Nakajima A, Gulick T, Chiche J-D, Orth D, de la Monte SM, Bloch KD.
588   Sp110 Localizes to the PML-Sp100 Nuclear Body and May Function as a Nuclear
589   Hormone Receptor Transcriptional Coactivator. Mol Cell Biol 2000; 20:6138–6146.

590   [33] Qi B, Sang RGN and Q-XA. ADAM19/Adamalysin 19 Structure, Function, and Role as
591   a Putative Target in Tumors and Inflammatory Diseases; 2009.
592   http://www.eurekaselect.com/69551/article. Accessed 20 August 2018.

593   [34] Hamazaki H, Hamazaki MH. Catalytic site of human protein-
594   glucosylgalactosylhydroxylysine glucosidase: Three crucial carboxyl residues were
595   determined by cloning and site-directed mutagenesis. Biochem Biophys Res Commun
596   2016; 469:357–362.

597   [35] Hammond ER, Stewart B, Peek JC, Shelling AN, Cree LM. Assessing embryo quality
598   by combining non-invasive markers: early time-lapse parameters reflect gene expression
599   in associated cumulus cells. Hum Reprod 2015; 30:1850–1860.

600   [36] Gauvin TJ, Young LE, Higgs HN. The formin FMNL3 assembles plasma membrane
601   protrusions that participate in cell-cell adhesion. Mol Biol Cell 2015; 26:467–477.

602   [37] Cesaro MD, Santos J dos, Ferst JG, Nóbrega JE, Rosa PRA, Rovani MT, Ilha GF,
603   Bohrer RC, Ferreira R, Gasperin BG, Bordignon V, Gonçalves PBD. Natriuretic peptide
604   system regulation in granulosa cells during follicle deviation and ovulation in cattle.
605   Reprod Domest Anim 2018; 53:710–717.

606   [38] Zheng Y-Z, Liang L. High expression of PXDN is associated with poor prognosis and
607   promotes proliferation, invasion as well as migration in ovarian cancer. Ann Diagn
608   Pathol 2018; 34:161–165.

609   [39] Luo C-W, Kawamura K, Klein C, Hsueh AJW. Paracrine Regulation of Ovarian
610   Granulosa Cell Differentiation by Stanniocalcin (STC) 1: Mediation through Specific
611   STC1 Receptors. Mol Endocrinol 2004; 18:2085–2096.

612   [40] Knight PG, Glister C. TGF-β superfamily members and ovarian follicle development.
613   Reproduction 2006; 132:191–206.

614   [41] Zhou X, Ren Y, Moore L, Mei M, You Y, Xu P, Wang B, Wang G, Jia Z, Pu P, Zhang
615   W, Kang C. Downregulation of miR-21 inhibits EGFR pathway and suppresses the
616   growth of human glioblastoma cells independent of PTEN status. Lab Invest 2010;
617   90:144–155.

618   [42] Yang L, Li Y, Wang X, Liu Y, Yang L. MicroRNA-320a inhibition decreases
619   insulin-induced KGN cell proliferation and apoptosis by targeting PCGF1. Mol Med
620   Rep 2017; 16:5706–5712.

621   [43] Friedman RC, Farh KK-H, Burge CB, Bartel DP. Most mammalian mRNAs are
622   conserved targets of microRNAs. Genome Res 2009; 19:92–105.

623   [44] van Montfoort APA, Plösch T, Hoek A, Tietge UJF. Impact of maternal cholesterol
624   metabolism on ovarian follicle development and fertility. J Reprod Immunol 2014; 104–
625   105:32–36.

626   [45] Tu K, Yu H, Hua Y-J, Li Y-Y, Liu L, Xie L, Li Y-X. Combinatorial network of primary
627   and secondary microRNA-driven regulatory mechanisms. Nucleic Acids Res 2009;
628   37:5969–5980.

629   [46] Khan AA, Betel D, Miller ML, Sander C, Leslie CS, Marks DS. Transfection of small
630   RNAs globally perturbs gene regulation by endogenous microRNAs. Nat Biotechnol
631   2009; 27:549–555.

632   [47] Grimson A, Farh KK-H, Johnston WK, Garrett-Engele P, Lim LP, Bartel DP.
633   MicroRNA Targeting Specificity in Mammals: Determinants Beyond Seed Pairing. Mol
634   Cell 2007; 27:91–105.

635   [48] Varendi K, Mätlik K, Andressoo J-O. From microRNA target validation to therapy:
636   lessons learned from studies on BDNF. Cell Mol Life Sci 2015; 72:1779–1794.

637   [49] Nilsson EE, Kezele P, Skinner MK. Leukemia inhibitory factor (LIF) promotes the
638   primordial to primary follicle transition in rat ovaries. Mol Cell Endocrinol 2002;
639   188:65–73.

640 [50] Ilha GF, Rovani MT, Gasperin BG, Antoniazzi AQ, Gonçalves PBD, Bordignon V,
641   Duggavathi R. Lack of FSH support enhances LIF–STAT3 signaling in granulosa cells
642   of atretic follicles in cattle. Reproduction 2015; 150:395–403.

643 [51] Andrade GM, da Silveira JC, Perrini C, Del Collado M, Gebremedhn S, Tesfaye D,
644   Meirelles FV, Perecin F. The role of the PI3K-Akt signaling pathway in the
645   developmental competence of bovine oocytes. PLoS ONE 2017; 12.

646 [52] Qu H, Sun H, Wang X. Neogenin-1 Promotes Cell Proliferation, Motility, and Adhesion
647   by Up-Regulation of Zinc Finger E-Box Binding Homeobox 1 Via Activating the
648   Rac1/PI3K/AKT Pathway in Gastric Cancer Cells. Cell Physiol Biochem 2018;
649   48:1457–1467.

650 [53] Zhao L, Du X, Huang K, Zhang T, Teng Z, Niu W, Wang C, Xia G. Rac1 modulates the
651   formation of primordial follicles by facilitating STAT3-directed Jagged1, GDF9 and
652   BMP15 transcription in mice. Sci Rep 2016; 6:23972.

653 [54] Ernst EH, Grøndahl ML, Grund S, Hardy K, Heuck A, Sunde L, Franks S, Andersen
654   CY, Villesen P, Lykke-Hartmann K. Dormancy and activation of human oocytes from
655   primordial and primary follicles: molecular clues to oocyte regulation. Hum Reprod
656   2017; 32:1684–1700.

657 [55] Chang H-M, Qiao J, Leung PCK. Oocyte–somatic cell interactions in the human
658   ovary—novel role of bone morphogenetic proteins and growth differentiation factors.
659   Hum Reprod Update 2016; 23:1–18.

660 [56] Mohan M, Thirumalapura NR, Malayer J. Bovine cumulus-granulosa cells contain
661   biologically active retinoid receptors that can respond to retinoic acid. Reprod Biol
662   Endocrinol RBE 2003; 1:104.

663 [57] Matsunaga E, Tauszig-Delamasure S, Monnier PP, Mueller BK, Strittmatter SM,
664   Mehlen P, Chédotal A. RGM and its receptor neogenin regulate neuronal survival. Nat
665   Cell Biol 2004; 6:749–755.

666 [58] Qi Y, Liu J, Saadat S, Tian X, Han Y, Fong G-H, Pandolfi PP, Lee LY, Li S. PTEN
667   induces apoptosis and cavitation via HIF-2-dependent Bnip3 upregulation during
668   epithelial lumen formation. Cell Death Differ 2015; 22:875–884.

669 [59] Noma N, Kawashima I, Fan H-Y, Fujita Y, Kawai T, Tomoda Y, Mihara T, Richards
670   JS, Shimada M. LH-Induced Neuregulin 1 (NRG1) Type III Transcripts Control
671   Granulosa Cell Differentiation and Oocyte Maturation. Mol Endocrinol 2011; 25:104–
672   116.

673 [60] Bai SW, Herrera-Abreu MT, Rohn JL, Racine V, Tajadura V, Suryavanshi N, Bechtel S,
674   Wiemann S, Baum B, Ridley AJ. Identification and characterization of a set of
675   conserved and new regulators of cytoskeletal organization, cell morphology and
676   migration. BMC Biol 2011; 9:54.

677 [61] Wolter JM, Kotagama K, Pierre-Bez AC, Firago M, Mangone M. 3'LIFE: a functional
678   assay to detect miRNA targets in high-throughput. Nucleic Acids Res 2014; 42:e132.

679

680

Figure Legends

Figure 1. Cluster analysis of gene expression changes upon transfection of KGN cells with cel-miR-39p, hsa-miR-548ba or hsa-miR-7973 miRNA mimic. Gene expression changes were analyzed 72 h after transfection on Affymetrix microarray. Only statistically significant results are presented (adjusted p-value < 0.01).

Figure 2. Validation of microarray results by RT-qPCR. A) Potential target genes of hsa-miR-548ba and B) Potential target genes of hsa-miR-7973. Gene expression change is calculated by comparing expression levels to samples transfected with control miRNA cel-miR-39-3p. Results are displayed as average fold change ±SD on $\log_2$ scale, ($^{\#}$p = 0.057, *p < 0.05; **p < 0.01; Student t-test). All presented microarray results were statistically significant (adjusted p < 0.01).

Figure 3. Validation of miRNA binding on the 3'UTR sequences of their potential target mRNAs by luciferase reporter assay. A) hsa-miR-548ba potential target genes. B) hsa-miR-7973 potential target genes. Results are shown as average normalized luciferase signal ±SEM, (*p < 0.05; **p < 0.01; Student one-tailed t-test). RLU – relative light unit.

Supplemental Data Legends

Supplementary Figure 1. Transient hsa-miR-548ba and hsa-miR-7973 expression in KGN cell-line compared to primary human granulosa cells. For positive control human mural (MGC) and cumulus granulosa cell (CGC) RNA was used (n=8). miRNA expression in KGN cells is shown as average expression of four parallel samples ± SD on $\log_2$ scale. miRNA expression

704   levels were normalized against miRNA hsa-miR-132-3p levels. Transfected KGN samples are

705   indicated with + sign in the legend (yellow and pink color).

706

707   **Supplementary Figure 2.** KGN cell viability upon transient miRNA expression.

708   Luminescence signal was measured from cells transfected with hsa-miR-548ba, hsa-miR-7973

709   or control miRNA cel-miR-39-3p at three time-points: 24, 48 and 72 hours. Signal from non-

710   transfected cells (control) were measured at 0, 24, 48 and 72 hours. The indicated value refers

711   to normalized luminescence: signal from all lysed cells minus signal from dead cells. Results

712   are shown as average of 3 independent experiment with ± SD. Student t-test p-values were

713   above 0.05, no significance difference in living cell number were detected between non-

714   transfected control samples and transfected cells.

715

716   **Supplementary Figure 3.** Suppression of luciferase signal upon hsa-miR-21-5p binding to

717   PTEN 3'UTR. pmirGLO-3'UTR-PTEN vector and hsa-miR-21-5p were used as a positive

718   control for miRNA:mRNA binding to confirm the luciferase assay reliability. Two versions of

719   PTEN 3'UTRs were used, pmirGLO-3'UTR-PTEN long represent 3'UTR length obtained

720   from UCSC genome browser and pmirGLO-3'UTR-PTEN short represents miRDB miRNA

721   target prediction program version of 3'UTR length. A) pmirGLO-3'UTR-PTEN long and B)

722   pmirGLO-3'UTR-PTEN short (*p < 0.05; Student t-test).

723

724   **Supplementary Table IA:** RT-qPCR primer table

725

726   **Supplementary Table IB:** Primers for amplifying 3'UTR sequences and restriction enzymes

727   used for pmirGLO-Dual luciferase vector cloning. With red is marked restriction enzyme

728   cutting sequences and with lowercase letters 5'overhang sequence

729   **Supplementary Table IIA**: Affymetrix microarray results upon KGN cell transfection with

730   hsa-miR-548ba, adjusted p-value <0.01

731

732   **Supplementary Table IIB**: Potential target genes of hsa-miR-548ba. Overlapping part of

733   Affymetrix microarray results (asjusted p-value <0.01) and bioinformatically predicted target

734   genes (predicted by at least 2 programs out of 4). Bioinformatical programs: DIANA microT

735   v3.0, microT CDS v5.0, TargetScan 7.1 and miRDB. Genes marked red were validated by RT-

736   qPCR.

737

738   **Supplementary table IIC:** Affymetrix microarray results upon KGN cell transfection with

739   hsa-miR-7973, adjusted p-value <0.01.

740

741   **Supplementary Table IID:** Potential target genes of hsa-miR-7973. Overlapping part of

742   Affymetrix microarray results (adjusted p-value <0.01) and bioinformatically predicted target

743   genes (predicted by at least 2 programs out of 4). Bioinformatical programs: DIANA microT

744   v3.0, microT CDS v5.0, TargetScan 7.1 and miRDB. Genes marked red were validated by RT-

745   qPCR.

746

747   **Supplementary Table IIIA:** Reactome pathways regulated upon transfection of KGN cell-

748   line with hsa-miR-548ba mimic. Pathways in bold are unique to hsa-miR-548ba regulation in

749   comparison to samples expressing hsa-miR-7973.

750

751   **Supplementary table IIIB:** Reactome pathways regulated upon transfection of KGN cell-line

752   with hsa-miR-7973 mimic. Pathways in bold are unique to hsa-miR-7973 regulation in

753   comparison to samples expressing hsa-miR-548ba.

754   **Supplementary Material.** Target gene 3'UTR sequences and bioinformatically predicted

755   target sites for miRNAs hsa-miR-548ba or hsa-miR-7973. Four target prediction programs

756   were used: DIANA microT v 3.0, microT CDS v5.0, TargetScan 7.1 and miRDB. Red

757   underlined sequences represent seed sequences predicted by both TargetScan and miRDB,

758   green underlined sequences represent microT CDS v.5.0 predicted target sequences, blue

759   underlined sequences represent only TargetScan predicted seed sequence location and yellow

760   marks seed sequences predicted only by miRDB. Hsa-miR-548ba potential target gene 3'UTRs

761   are: a) BCL2L11, b) LIFR, c) NEO1, d) PTEN, e) RARB and f) SP110. Hsa-miR-7973

762   potential target gene 3'UTRs are: g) ADAM19, h) ATHL1 i) ATP6V1A, j) FMNL3 and k)

763   PXDN. Potential target gene for both hsa-miR-548ba and hsa-miR-7973 3'UTR is: k)

764   TGFBR2.

765

766

767

768

769

770

771

772

773

774

775

776

777

778

Table I. Potential target genes of hsa-miR-548ba and hsa-miR-7973 used in validation studies and their cellular functions.

Potential hsa-miR-548ba target genes

Gene symbol	Gene name	Cellular function	Reference
BCL2L11	BCL2 Like 11	BCL-2 family activator of apoptosis.	[25]
GALNT7	Polypeptide N-Acetylgalactosaminyltransferase 7	Androgen-dependent GalNAc-transferase involved in mucin-type O-linked protein glycosylation.	[26]
INSIG1	Insulin Induced Gene 1	Regulates cholesterol synthesis.	[27]
LIFR	LIF Receptor Alpha	Growth initiation of human primordial follicles.	[28]
NEO1	Neogenin 1	Binds directly bone morphogenetic proteins (BMPs).	[29]
PTEN	Phosphatase And Tensin Homolog	Activation of primordial follicles from the dormant pool.	[30]
RARB	Retinoic Acid Receptor Beta	Nuclear receptor regulating the transcription of steroidogenic genes in the ovary.	[31]
SP110	SP110 Nuclear Body Protein	Nuclear hormone receptor coactivator, enhances retinoic acid receptor signal.	[32]

Potential hsa-miR-7973 target genes

Gene symbol	Gene name	Cellular function	Reference
ADAM19	ADAM Metallopeptidase Domain 19	Cleaves extracellular matrix (ECM) proteins	[33]
ATHL1	Acid Trehalase-Like Protein 1	Cleaves ECM protein collagen.	[34]
ATP6V1A	ATPase H+ Transporting V1 Subunit A	Involved in energy metabolism, expression correlates with human embryo quality.	[35]
FMNL3	Formin Like 3	Involved in cell-cell adhesion.	[36]
NPR3	Natriuretic Peptide Receptor 3	Maintains oocyte meiotic arrest.	[37]
PXDN	Peroxidasin	ECM protein with peroxidase activity.	[38]
STC1	Stanniocalcin 1	Regulates phosphate metabolism, potential luteinization inhibitor.	[39]

Potential hsa-miR-548ba and hsa-miR-7973 target gene

Gene symbol	Gene name	Cellular function	Reference

	TGFBR2	Transforming Growth Factor Beta Receptor 2	Intercellular communication during ovarian follicle development.	[40]

779

780

781

782

783

784

785

786

787
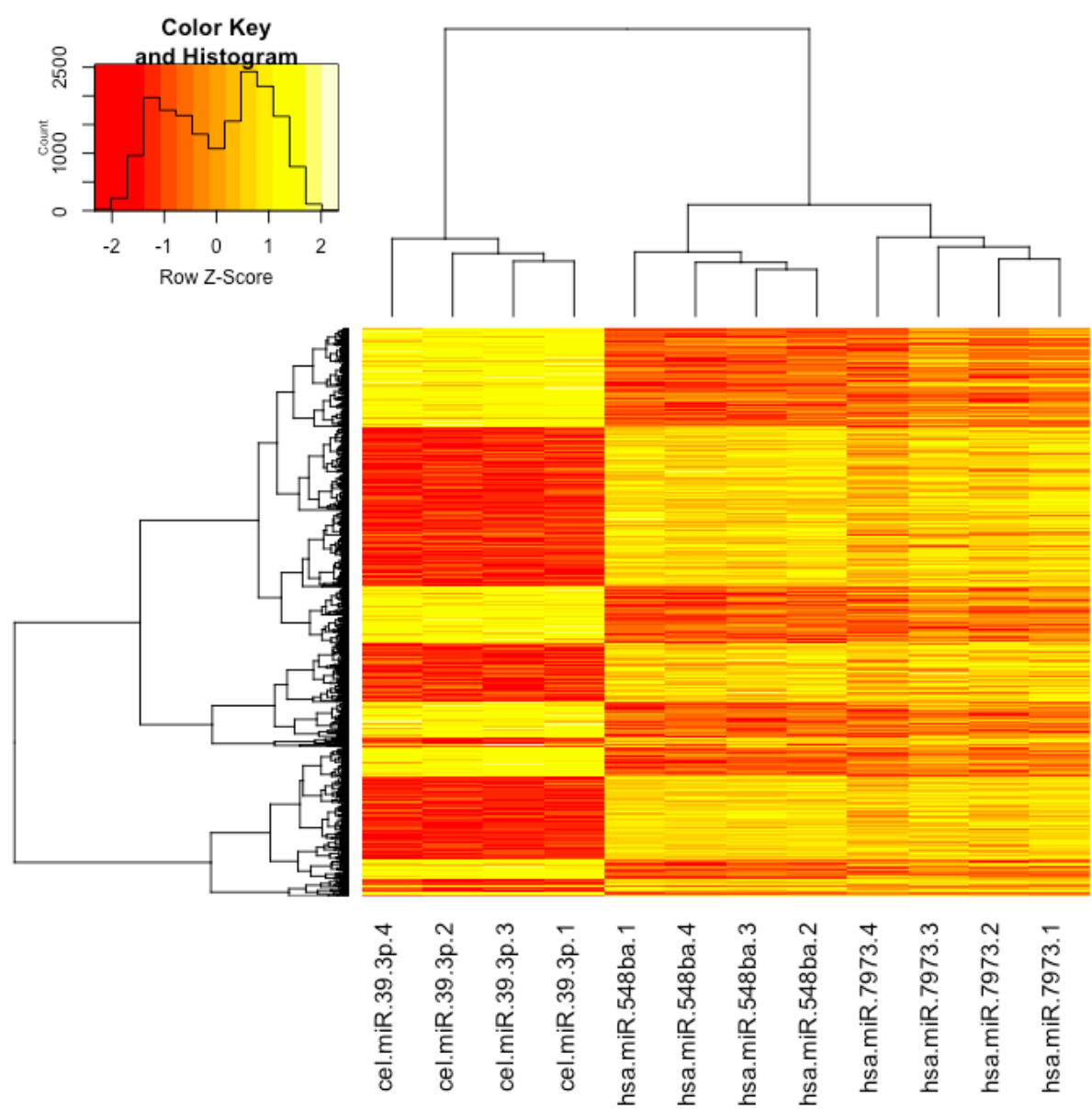
788

789
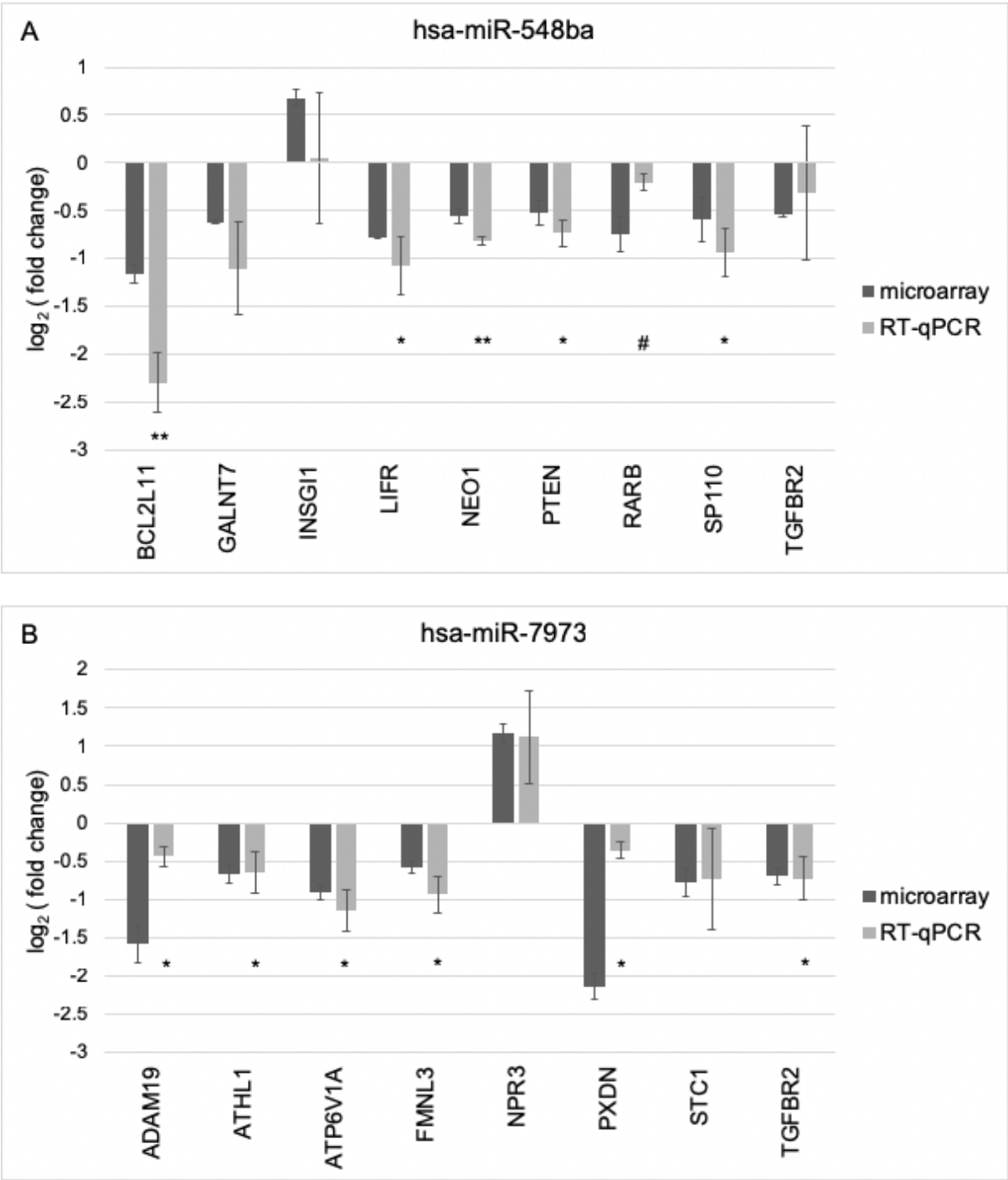
790
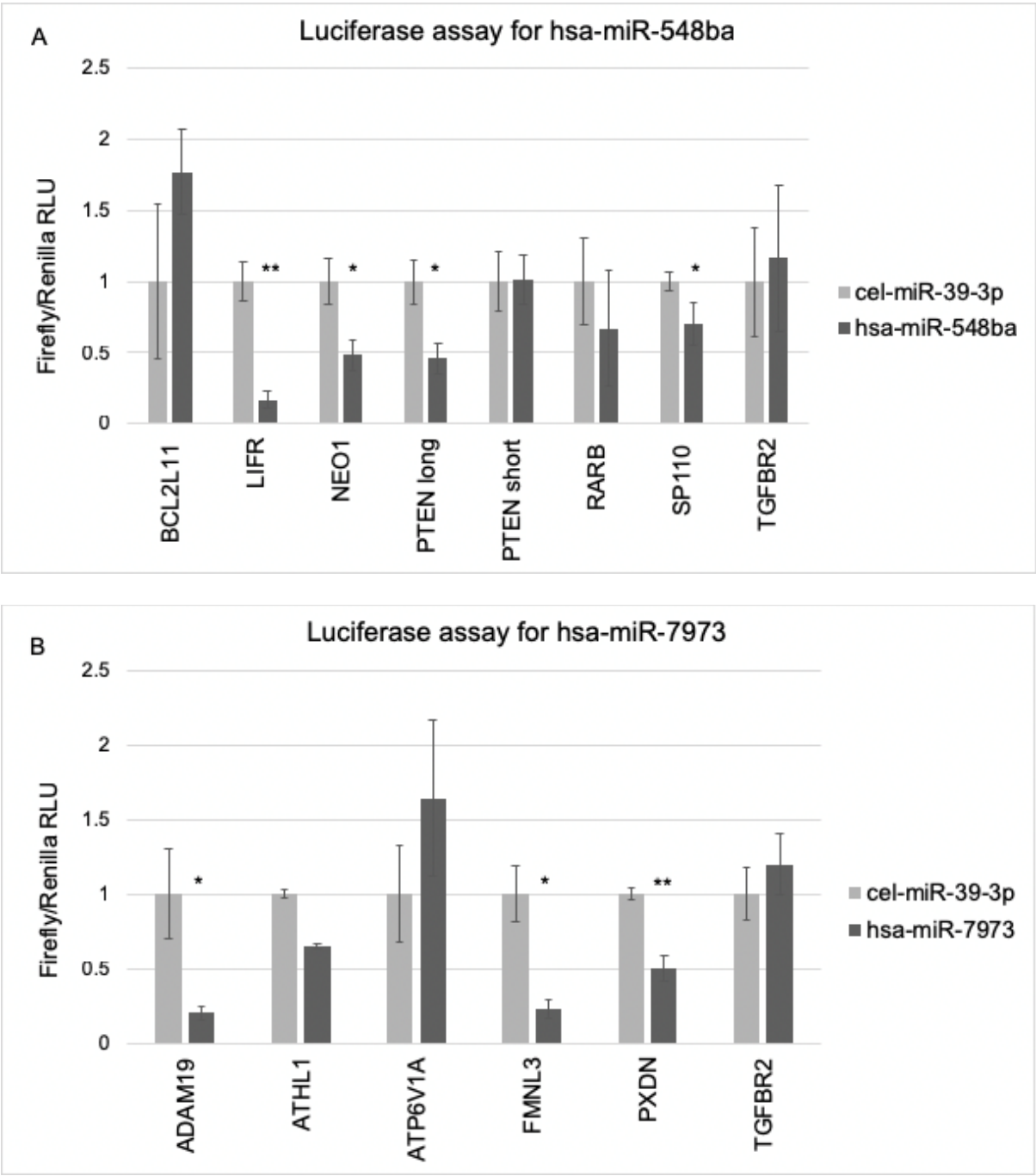
791

792

793

794

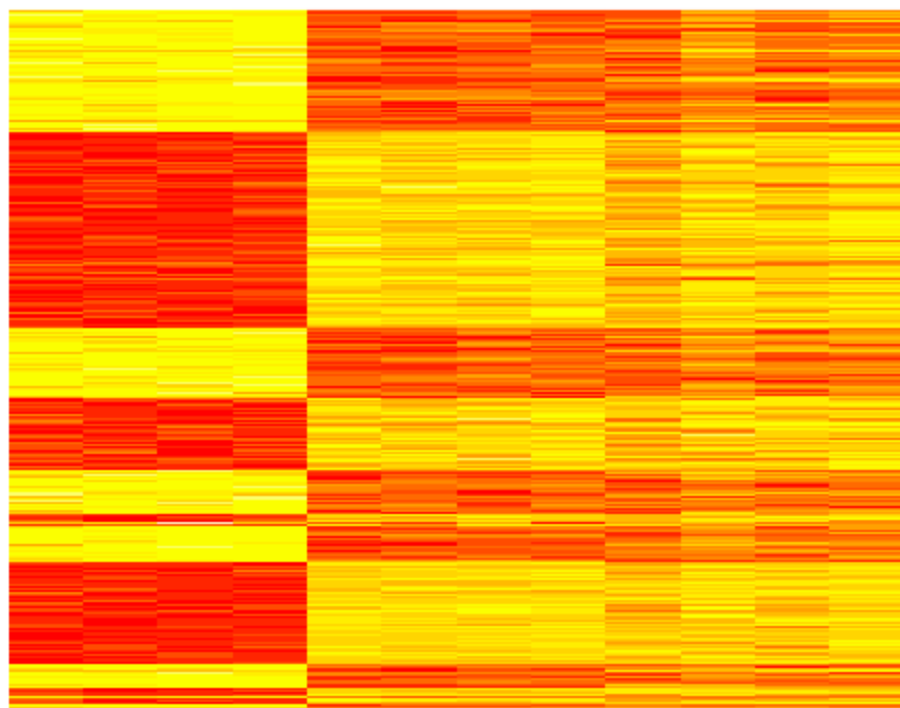795

796

797

798

799

800

801

802
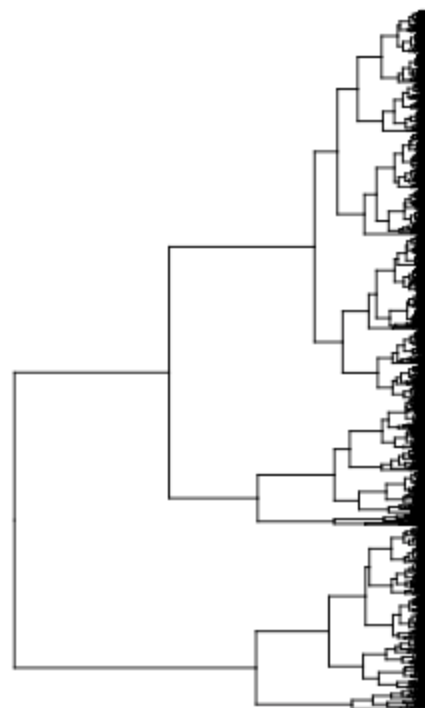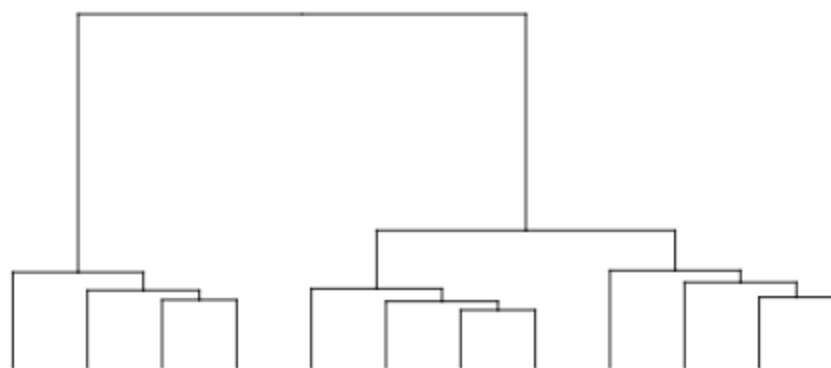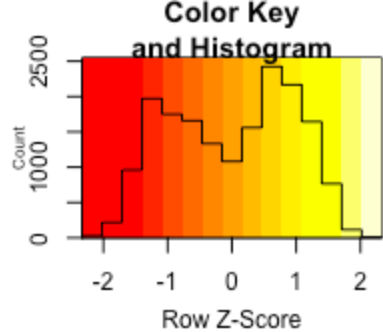
803   **Figure 1.**

804

805

806

807

808

809

810

811

812   **Figure 2.**

813

814

815

816

817

818

819

820 **Figure 3.**

821

822

823

824

A
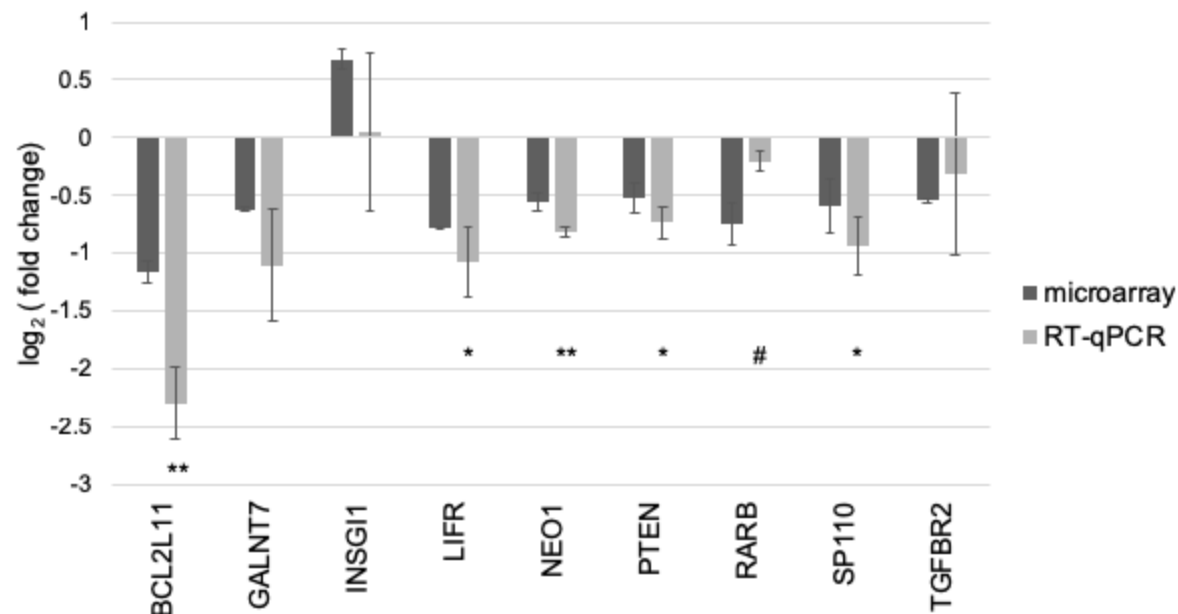
hsa-miR-548ba

B

hsa-miR-7973
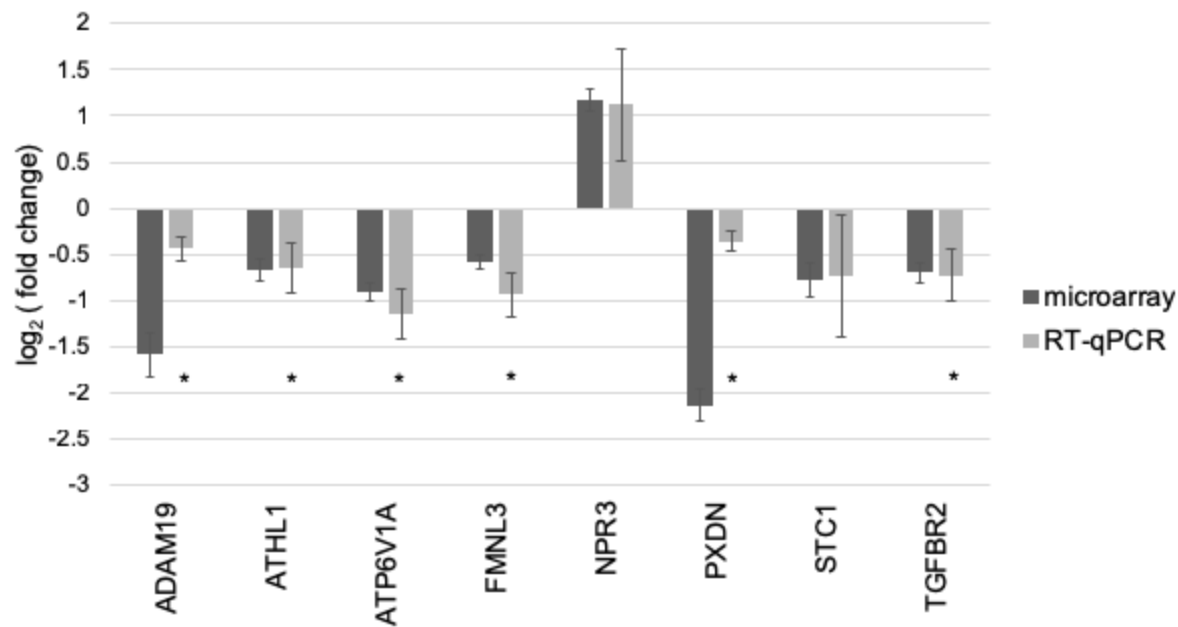
A Luciferase assay for hsa-miR-548ba

(Firefly/Renilla RLU vs. BCL2L11, LIFR, NEO1, PTEN long, PTEN short, RARB, SP110, TGFBR2; cel-miR-39-3p and hsa-miR-548ba; LIFR: **, NEO1: *, PTEN long: *, SP110: *)

B Luciferase assay for hsa-miR-7973

(Firefly/Renilla RLU vs. ADAM19, ATHL1, ATP6V1A, FMNL3, PXDN, TGFBR2; cel-miR-39-3p and hsa-miR-7973; ADAM19: *, FMNL3: *, PXDN: **)